

SI Text

## **Methods**

### *Cell lines and cultures*

Human primary melanocytes were prepared from discarded foreskins and maintained in TICVA media (F-12 media with penicillin/streptomycin/glutamine, 7.5% FBS, 50ng/mL TPA, 225 $\mu$ M IBMX, 1 $\mu$ M Na<sub>3</sub>VO<sub>4</sub> and 1mM dbcAMP). WM1575 and WM3619 were grown in Tu-2% media (80% MCDB153 media, 20% Leibovitz's L-15 media), supplemented with 2% fetal bovine serum, 5 $\mu$ g/ml bovine insulin, and 1.68mM calcium chloride. All other cell lines were grown in RPMI or DMEM media supplemented with 10% fetal bovine serum. All cell lines were propagated at 37°C and 5% CO<sub>2</sub> in humidified atmosphere. Cell number was estimated by crystal violet staining followed by extraction with acetic acid and measurement at 405nm using a spectrophotometer.

### *Western blotting and immunohistochemistry*

For western blotting, whole cell lysates were collected in lysis buffer containing PBS/1% Triton X-100 and supplemented with protease and phosphatase inhibitors (Roche). Centrifuged supernatants normalized for protein content (Bio-Rad). Equal amounts of protein were resolved by electrophoresis on 4-15% or 10-20% gradient gels and transferred to nitrocellulose membranes. Quantification of BCL2A1 protein was performed using NIH ImageJ software.

The Skin SPORE melanocytic tumor progression tissue microarray (1, 2) contains four hundred and eighty 0.6mm diameter formalin-fixed paraffin embedded tissue cores of benign nevi (n=132 cores), primary cutaneous melanomas (n=198 cores), lymph node metastasis (n=58) and metastases to viscera (n=92). Five micrometer histologic sections

were cut using a rotary microtome and mounted on Fisher Superfrost plus slides using a paraffin tape-transfer system (Instrumedics, Inc., St Louis, MO). and the Dako Cytomation Kit (Glostrup, Denmark) using heated 10mM sodium citrate antigen retrieval buffer. Controls included omission of primary antibody. Slides were counterstained with hematoxylin and dehydrated in ethanol to xylene. The intensity of staining was scored visually by E.B.H. and L.M.D. as follows: 0, no staining and no background, 1 for weak bluish of staining (required 40X to distinguish from absent expression), 2 for clear, moderate staining or strong staining of < 50% of tumor cells, and 3 for intense staining of more than 50% of tumor cells. Statistical analysis was done by the Students' t-test.

### *Biostatistical Analysis*

A tissue microarray (TMA) with melanoma with known clinical and pathology annotation was used to correlate BCL2A1 expression with prognosis. Details of the TMA construction, respective control tissues has been previously described (3). Briefly, 160 Stage III melanoma metastases were assembled into a TMA. Each was categorized as either good overall survival (>5 years; n=80) or poor survival (<2 years, n=80). All negative control tissues showed no staining and positive control tissues were positive. Scoring of staining (by E.H. and L.M.D.) and bio statistical analysis was doubled-blinded. Chi-Square test was used in examining the association between categorical variables. Student t-test was used in comparing means of two continuous variables. Log rank test was used in comparing disease specific survival curves and disease free survival curves generated by Kaplan Meier Methods. The variables were presence of ulceration; age at diagnosis (>50 versus  $\leq$  50 years); BCL2A1 staining (2,3 versus 0,1); and number of positive lymph nodes (1 versus 2-3 versus  $\geq$  4). Variables that showed P-value < 0.1 in initial invariable analyses were entered into multivariable Cox proportional hazard model (Cox PH model). In selecting the best parsimonious model as a final model, both forward

selection and backward elimination methods were used using  $p$ -values of 0.05 as a selection/elimination criteria. The final Cox PH model for disease specific survival included number of positive lymph nodes ( $p = 0.002$ ) and BCL2A1 staining ( $p = 0.0296$ ). The final model for disease-free survival was an univariable model that included the number of positive lymph node ( $p = 0.053$ ). The validity of proportional hazard assumption on the final models was examined by Cox Snell residual plot.  $P$ -value  $\leq 0.05$  was considered statistically significant. All the analyses were done using SAS 9.0 (Cary, NC).

*BCL2A1* mRNA, normalized to *ACTB*, was quantified by real-time PCR in patients who had best overall RECIST responses  $> 30\%$  to BRAF pathway inhibitors (see SI Appendix, Table S4) versus those without objective responses. Based on expected *BCL2A1* expression to be less in the patients with objective response, a two-sample  $t$ -test was performed assuming unequal variance.

#### *Bioinformatic analysis*

The Affymetrix expression data for 319 GSK cancer cell lines (<https://array.nci.nih.gov/caarray/project/woost-00041>) and 72 normal tissue samples (GNF) (4) were normalized together using RMA (5) and adjusted for batch effects based on empirical Bayes methods (6). Each cancer group was compared to the pooled set of GNF normal tissues by applying the algorithm Differential Expression via Distance Synthesis (7), which combines  $t$ -test, moderated  $t$ -test, Significance Analysis of Microarrays, and fold-change into a single statistic. For melanoma, 73 genes were significantly higher in melanoma compared to normal tissues at 0% False Discovery Rate (FDR). Then 784 genes that were both amplified in melanoma at a GISTIC  $q$ -value cutoff of  $10^{-5}$  (8) and showed significant differential expression in melanoma at 5%  $q$ -value cutoff (8, 9) were considered, according to the  $t$ -test of expression levels between

amplified melanoma samples and normal melanocytes. This analysis was applied to other cancers using the recent copy number profiles of cancer genomes (10).

Clustering analysis was done using Gene Pattern (11). For analysis of the 15q amplicon, we observed that within a given sample, the rounded CNA number stayed the same along the chromosome 15q region, with only very few exceptions, and the variation in the GISTIC values were attributable to the fact that the computed CNA numbers were floating point and could thus depend on the algorithm for inferring CNA from the SNP data. Expression data were available for 88 melanoma samples with matching copy number analysis data and 5 melanocyte samples (8, 12). The differential expression level of the 225 candidate RefSeq genes between 15q amplified samples and unamplified samples was computed. For MITF-regulated genes, as determined by shRNA knockdown, we excluded from the control set those samples with MITF amplification on chromosome 3. The expression data had a clear bimodal distribution, separating undetectable or lowly expressed genes from highly expression ones. Some differentially expressed amplified genes thus had only very limited absolute expression and were unlikely candidates of oncogenic activities. Consequently, genes with an amplified expression index less than 6.44 were filtered out, which corresponds to the intersection point of the two lowest components in a mixture model of three normal distributions, and those with a differential expression  $p$ -value greater than 0.05 using the Wilcoxon Rank Sum Test.

BCL2A1 mRNA expression was compared to the expression of all known and sequence-predicted human transcription factors (<http://dbd.mrc-lmb.cam.ac.uk/DBD/index.cgi?Home>) by Pearson correlation analysis using the GeneNeighbors module of Gene Pattern. Mathematical details are provided at <http://www.broad.mit.edu/webservices/gpModuleRepository/download/prod/module/?file>



=/GeneNeighbors/broad.mit.edu:cancer.software.genepattern.module.analysis/00007/2/  
GeneNeighbors.pdf).

*RNA isolation, chromatin immunoprecipitation and quantitative real-time PCR*

All real-time PCR experiments were done in at least triplicate with three independent experiments. Primers used were hBCL2A1\_QF1, CCCGGATGTGGATACCTATAAGGAGA; hBCL2A1\_QR1 GTCATCCAGCCAGATTTAGGTTCA; hM-MITF-QF1-770, CATTGTTATGCTGGAAATGCTAGAA; hM-MITF-QR1-771, GGCTTGCTGTATGTGGTACTTGG. Results were normalized to *ACTB*. Chromatin immunoprecipitation (ChIP) was performed in MALME-3M human melanoma cells as previously described (13). Chromatin was immunoprecipitated using rabbit anti-MITF (polyclonal), or normal rabbit IgG (Santa Cruz) as a control. Quantitative PCR was performed on samples using primers for *BCL2A1* -7kb region (forward primer, 5'-AAGGCATAGTGA CTGGACTGCCAT-3' and reverse primer, 5'-TCACCCTGATTACGAAACAGGCCA-3'), *BCL2A1* 5'-UTR region (forward, 5'-ACA GCC TAC GCA CGA AAG TGA CTA-3') and reverse, 5'-TGA AGC TGT TGA GGC AAT GTG CTG-3'), hTYR (forward, 5'-GTG GGA TAC GAG CCA ATT CGA AAG-3') and (reverse, 5'-TCC CAC CTC CAG CAT CAA ACA CTT-3'), and *ACTB* (forward, 5'-CAT CCT CAC CCT GAA GTA CCC-3' and reverse, 5'-TAG AAG GTG TGG TGC CAG ATT-3').

Genomic DNA was isolated using DNeasy Blood & Tissue Kit (Qiagen). Primers used copy number analysis were hBCL2A1\_CIF2, TGAACCTAAATCTGGCTGGATGAC; hBCL2A1\_CIR2, GGCCGGTTTCACAATATGGAGTGT; hLINE-1\_QF1, AAAGCCGCTCAACTACATGG; hLINE-1\_QR1, TGCTTTGAATGCGTCCCAGAG. The comparative cycle threshold method was used to quantify target gene or mRNA copy numbers in the samples.

Results were normalized to the repetitive element LINE-1 as described previously<sup>21</sup>.

The relative target copy number level was normalized to normal human genomic DNA as calibrator. Unless indicated, data presented are averages and standard error of at least three independent experiments.

#### *siRNA delivery and analysis*

shRNAs targeting BCL2A1, MITF or non-template control were from The RNAi Consortium (Broad Institute, Cambridge, MA USA). Lentivirus was packaged in 293T cells per standard protocols. Amount of virus was titrated for near quantitative infection with <5% toxicity of non-template virus. For lentiviral delivery, 1800 cells were plated on Day 1 in 96 well plates, infected on the following day, and cells were selected in 1µg/mL puromycin. Pooled siRNAs targeting MITF (catalog number M-008674-00-005, Dharmacon), BCL2A1 (L-003306-00-0005, Dharmacon) or individual siRNAs targeting BCL2A1 (LU-003306-00-0002, Dharmacon) or control siRNA were transfected at final concentration of 25nM using the lipidoid delivery agent C12-113-B (14). Lipidoid material was synthesized by reaction of 1,2-epoxydodecane with 2,2'-diamino-N-methyldiethylamine in a glass scintillation vial for 3 days at 90°C. Following synthesis, reaction mixture was characterized by MALDI-TOF mass spectroscopy to confirm mass of expected products. Reaction product was used for transfection without further purification. Lipidoid was dissolved in 25mM NaOAc buffer (pH~5.2) and added to solution of siRNA for complexation. Complexes of siRNA (final concentration of 25nM) were plated in 96 well plates, followed by plating of cells in growth media as above. Growth and knockdown efficiency (assessed by quantitative PCR) was measured after 48-72 hours.

For the effects of siRNA on resistance to prolonged PLX4720, M14 cells were plated at low density along with siControl or siBCL2A1. The following day, media was

replaced with media containing PLX4720 (20 $\mu$ M) for 2 weeks. Cell number was determined after staining with crystal violet above.

#### *Mouse xenotransplantation*

Melanoma cells were infected with lentivirus expressing shBCL2A1 or control virus, selected with puromycin as above. The cells were injected into nu/nu mice at 48hrs or harvested at 72hrs for Western blot analysis for knockdown validation. For mouse xenotransplant experiments,  $1 \times 10^7$  cells were injected subcutaneously into the flanks of female nu/nu mice. After 12 days, mice were treated with chow containing PLX4720 (417 mg/kg per animal weight, roughly 30 or 60 mg/kg dose) or control. Obatoclax (5mg/kg) was administered by oral gavage 5 days per week. Tumor volume was calculated by the formula  $\frac{1}{2} \times (\text{length} \times \text{width}^2)$  by on the first and twelfth day of treatment, and was depicted as mean tumor volume per group. Percentage tumor growth inhibition was determined as  $(1 - (T/N)) \times 100$ , in which  $T$  is the mean change in tumor volume of the treated group and  $N$  is the mean change in tumor volume of the control group at the assay end-point. Two-tailed t-test calculations were performed using Prism 4 (GraphPad). All experiments were done in accordance to the NIH Guide to the Care and Use of Laboratory Animals and institutional guidelines.

#### *Effect of forskolin on BCL2A1 and MITF targets*

Twenty-four hours after plating primary melanocytes in TICVA media, media was washed, removed, and replaced with F-10 media with 3% fetal calf serum. Sixteen hours later, cells were stimulated with forskolin (20 $\mu$ M, diluted in ethanol) or vehicle control. Variability in the response to forskolin was observed among different donors; results shown are representative of at least three donors performed in triplicate.

### *Promoter assays and luciferase experiments*

The *BCL2A1* promoter was cloned into the pGL3-Basic vector (Promega) using primers as follows: 7kb *BCL2A1* promoter , h*BCL2A1*\_pF1, 5'-

GGGGATCCCCAGTCAGCGTTTATCATGTGCTTAGCATATGGCAGTCCAG-3' and

h*BCL2A1*\_pR, 5'-TGCCATGGTCTGCCTGGTGGAGAGCAAAGTCTTGAGC-3'.

Mutagenesis was performed using the QuickChange Mutagenesis Kit (Stratagene), resulting in mutation of the underlined sequence to GAAGTG. UACC-62 melanoma cells were transfected with the indicated promoter along with pRL-CMV *Renilla* control. At 48 hrs, luciferase readings were made using the Dual Luciferase Reporter Assay (Promega). Firefly luciferase values were normalized to *Renilla* luciferase. Results reported are the average of three independent experiments done in triplicate.

## SI Figure and Table Legends

Figure S1. Bio-informatics analysis of melanomas. (a) Expression of genes highly expressed in melanoma compared to pooled expression in 72 normal tissues. (b) GISTIC scores for *BCL2A1* amplification in melanoma and other cancer types. Genes highly expressed in melanoma relative to normal tissue types are in red (c-d) GISTIC analysis of copy number of *BCL2A1* in melanomas from (c) Broad Institute collection (8) and (d) Sanger Institute collection. (e) Comparison of the mRNA expression of chromosome 15 amplicon genes, including *BCL2A1* and 224 others, in amplified versus non-amplified cell lines. The expression data had a clear bimodal distribution, separating undetectable or lowly expressed genes from highly expression ones. Consequently, genes with an amplified expression index less than 6.44 were filtered out, which corresponds to the intersection point of the highest mixture component with the remainder, and those with a differential expression  $p > 0.05$  using the Wilcoxon Rank Sum test.

Figure S2. Expression level of *MITF* and *BCL2A1* in normal skin and melanoma. *BCL2A1* and *MITF* mRNA expression levels from normal skin and melanoma were extracted from (15), normalized and transformed to log<sub>2</sub> scale as described in SI Text.

Figure S3. Expression of *BCL2A1* is related to copy number. (a) Quantification of *BCL2A1* copy number in primary melanocytes and melanomas by genomic PCR. (b) Log *BCL2A1* mRNA expression of 88 short-term melanoma cultures (8) was compared to inferred copy number for *BCL2A1* as described in SI Text. (c) Protein expression of *BCL2A1* in cells transfected with si*BCL2A1* or control siRNA, 72 hours after transfection. The blot was stripped and reprobred to detect expression of GAPDH as a loading control.

(d) Quantification of baseline BCL2A1 protein, normalized to GAPDH in melanoma cell lines shown in (a) with or without 15q amplification.

Figure S4. Knockdown efficiency of siRNAs targeting 15q amplicon candidates. M14 cells were transfected with siRNA targeting each of the indicated genes. (a) mRNA or (b) protein expression was detected after 72hrs. **\*\*\***,  $p < 0.001$  relative to control. (c) Requirement of candidate 15q oncogenes in growth of 501mel cell line. Cells were transfected with siRNA and cell number was estimated by crystal violet staining at 72hrs post-transfection. (d) Expression of BCL2A1 72h after infection of M14 cells with shRNA targeting BCL2A1.

Figure S5. Anti-BCL2A1 antibody stains melanoma specifically. (a) Representative melanoma section stained with anti-BCL2A1 antibody. BCL2A1 staining was observed in melanoma but not surrounding stroma. (b) Tissue staining intensity scores as described in Methods. These four cases of melanoma display the range of intensity of staining for BCL2A1.

Figure S6. Assessment of BCL2A1 protein expression in AJCC Stage III melanoma patients. (a) Table of summary of univariate and multivariate analysis. The multivariate analysis of known prognostic variables included ulceration, Breslow thickness, age at diagnosis (> 50 years or not), BCL2A1, and number of positive regional lymph nodes. Kaplan-Meier survival curves for disease-free survival (b) and melanoma-specific survival (c) are shown.

Figure S7. (a) MITF overexpression induces *BCL2A1* expression in transformed melanocytes. Pmel\* BRAF(V600E) cells were infected with lentivirus expressing green fluorescent protein or *M-MITF*. *BCL2A1* mRNA (left) or MITF protein (right) were evaluated by real-time PCR or Western blot respectively. (b) Effect of knockdown of MITF using two different shRNAs on anti-apoptotic BCL2 family in UACC-62 melanoma cells or primary melanocytes. mRNA for each BCL2 family member was quantified by real-time PCR 96 hours after infection with shRNA (UACC-62 cells) or 72 hours after transfection of siRNA (melanocytes) (c) Distribution of the RNA-seq expression values (16) of MITF-regulated vs. not regulated genes, based on responsiveness to MITF overexpression (17).

Figure S8. Amplification of BCL2 family members in melanoma and other cancers. Each gene was evaluated for amplification using GISTIC. Black denotes amplification at 1%  $q$ -value cutoff.

Figure S9. Role of BCL2A1 in resistance to PLX4720. (a) UACC62 cells ectopically expressing BCL2A1 or vector control treated with indicated dose of PLX4720 or vehicle. Cell number was estimated by Cell-Titer Glo. (b) Representative cell lines with or without BCL2A1 amplification were treated with siBCL2A1 or vehicle and indicated dose of PLX4720. Cell number was estimated by Cell-Titer Glo. (c) Effect of two week long treatment of M14 cell line with PLX4720 (20 $\mu$ M) transfected with siBCL2A1 or control siRNA. Representative photograph of cells following crystal violet staining (top). Average cell number was quantitated after crystal violet staining (bottom). \*\*\*\*,  $p < 0.0001$  compared to siControl. (d) MALME or (e) UACC257 cells transfected with siMITF and treated as described in (b). (f) (top) Effect of individual siRNAs targeting BCL2A1 on

sensitivity of M14 cells to PLX4720 ( $3\mu\text{M}$ ). Apoptosis was evaluated by Annexin V staining after 72 hrs of drug treatment. (bottom) Effect of individual siRNAs targeting BCL2A1 after on BCL2A1 mRNA at 72 hours. (g) Effect of pooled siRNA targeting BCL2A1 on BCL2A1 protein in M14 and MeWo cells, 72 hrs after transfection.

Figure S10. Resistance to PLX4720 mediated by overexpression of BCL2A1. (a) Effect of BCL2A1 overexpression in A375 melanoma cells on cell cycle. Propidium iodide flow cytometry was used to determine cell cycle 72 hours after treatment with  $3\mu\text{M}$  PLX4720. (b) Effect of PLX4720 on cell cycle markers and cleaved PARP in A375 cells expressing BCL2A1 or empty vector, at 72hrs post-treatment. (c) Effect of siRNA targeting BCL2A1 on cell cycle 72 hours after transfection in M14 and 501mel cells. Below is shown Western blot of BCL2A1 protein 72 hours after transfection of siRNA. (d) Effect of BCL2A1 overexpression on sensitivity to GSK1120212 at indicated dose. Cell number was estimated 72 hours after treatment with Cell Titer Glo. (e) Effect of BCL2A1 overexpression on sensitivity of A375 to cisplatin or etoposide, 72 hours after treatment.

Figure S11. Effect of obatoclox *in vitro* and *in vivo*. (a) Apoptosis following 48h treatment of UACC257 or A375P cells treated with PLX4720 ( $3\mu\text{M}$ ), obatoclox (100nM) or both. (b) Average weight of mice treated in Figure 5(h) following 2 week treatment with PLX4720 or PLX4720 with obatoclox.

Table S1. Genes expressed at higher levels in cancer compared to normal tissues.

Genes from melanoma, breast cancer, colorectal cancer, lung cancer, medulloblastoma, and glioblastoma are presented. DEDS (Differential Expression via Distance Synthesis),



log fold change, Significance Analysis of Microarrays (SAMS), and moderated t-test were calculated as described in the Methods.

Table S2. Bioinformatics analysis comparing mRNA expression of all transcription factors to BCL2A1 mRNA in 88 short-term melanoma cell lines. The most highly correlated transcription factors by Pearson correlation are listed.

Table S3. BRAF mutation and BCL2A1 amplification of cell lines used in this manuscript.

Table S4. Patients biopsied and evaluated for expression of BCL2A1 prior to indicated treatment. *BCL2A1* mRNA was calculated from biopsies of the patients listed.

## Supplemental References

1. Kim M, *et al.* (2006) Comparative oncogenomics identifies NEDD9 as a melanoma metastasis gene. *Cell* 125(7):1269-1281.
2. Nazarian RM PP, Lazar A, Elder D, Murphy G, Rimm D, Duncan LM. (2010) Protein Expression Signatures in Melanocytic Tumor Progression: A Tissue Microarray Study. *Journal of Cutaneous Pathology* 37:41-47.
3. Nguyen T, *et al.* (2011) Downregulation of microRNA-29c is associated with hypermethylation of tumor-related genes and disease outcome in cutaneous melanoma. *Epigenetics* 6(3):388-394.
4. Su AI, *et al.* (2004) A gene atlas of the mouse and human protein-encoding transcriptomes. *Proc Natl Acad Sci U S A* 101(16):6062-6067.
5. Irizarry RA, *et al.* (2003) Exploration, normalization, and summaries of high density oligonucleotide array probe level data. *Biostatistics* 4(2):249-264.
6. Johnson WE, Li C, & Rabinovic A (2007) Adjusting batch effects in microarray expression data using empirical Bayes methods. *Biostatistics* 8(1):118-127.
7. Yang YH, Xiao Y, & Segal MR (2005) Identifying differentially expressed genes from microarray experiments via statistic synthesis. *Bioinformatics* 21(7):1084-1093.
8. Lin WM, *et al.* (2008) Modeling genomic diversity and tumor dependency in malignant melanoma. *Cancer research* 68(3):664-73.

9. Storey JD (2002) A direct approach to false discovery rates. *Journal of the Royal Statistical Society Series B-Statistical Methodology* 64:479-498.
10. Beroukhim R, *et al.* (2010) The landscape of somatic copy-number alteration across human cancers. *Nature* 463(7283):899-905.
11. Reich M, *et al.* (2006) GenePattern 2.0. *Nature genetics* 38(5):500-501.
12. Thomas RK, *et al.* (2007) High-throughput oncogene mutation profiling in human cancer. *Nature Genetics* 39(17293865):347-351.
13. Du J, *et al.* (2004) Critical role of CDK2 for melanoma growth linked to its melanocyte-specific transcriptional regulation by MITF. *Cancer cell* 6(15607961):565-576.
14. Mahon KP, *et al.* (2010) Combinatorial approach to determine functional group effects on lipidoid-mediated siRNA delivery. *Bioconjug Chem* 21(8):1448-1454.
15. Talantov D, *et al.* (2005) Novel genes associated with malignant melanoma but not benign melanocytic lesions. *Clinical cancer research : an official journal of the American Association for Cancer Research* 11(16243793):7234-7242.
16. Berger MF, *et al.* (2010) Integrative analysis of the melanoma transcriptome. *Genome Res* 20(4):413-427.
17. Hoek KS, *et al.* (2008) Novel MITF targets identified using a two-step DNA microarray strategy. *Pigment Cell Melanoma Res* 21(6):665-676.

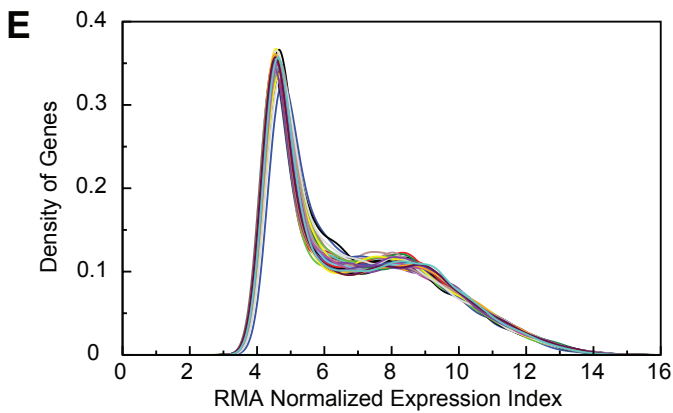
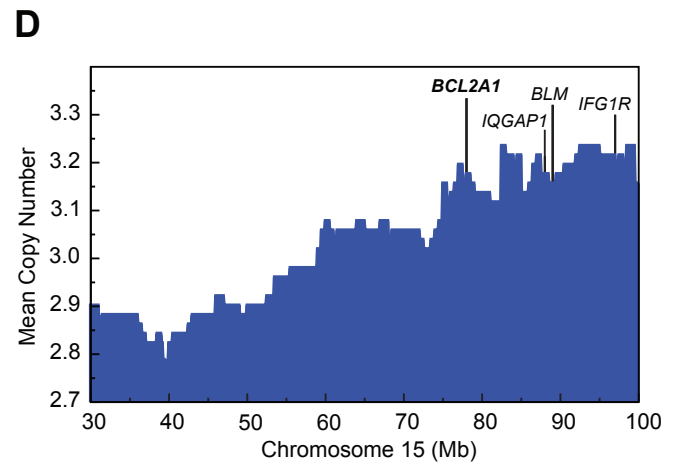
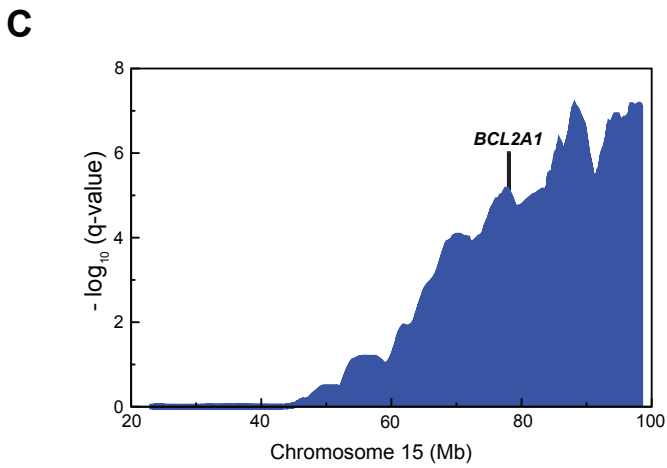
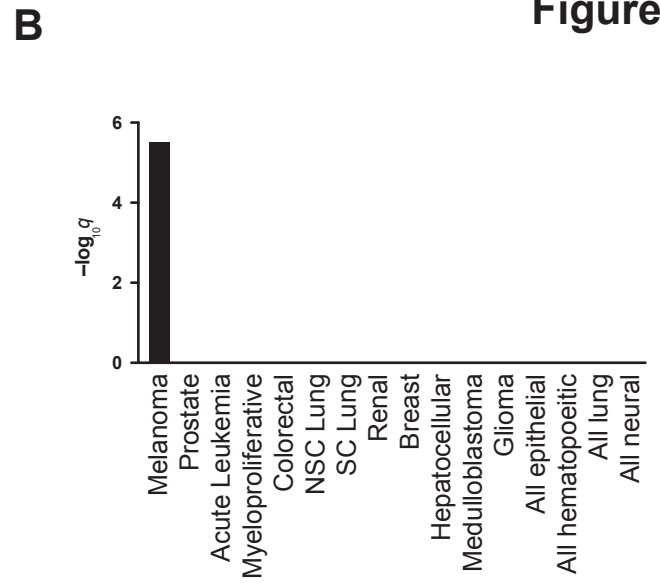
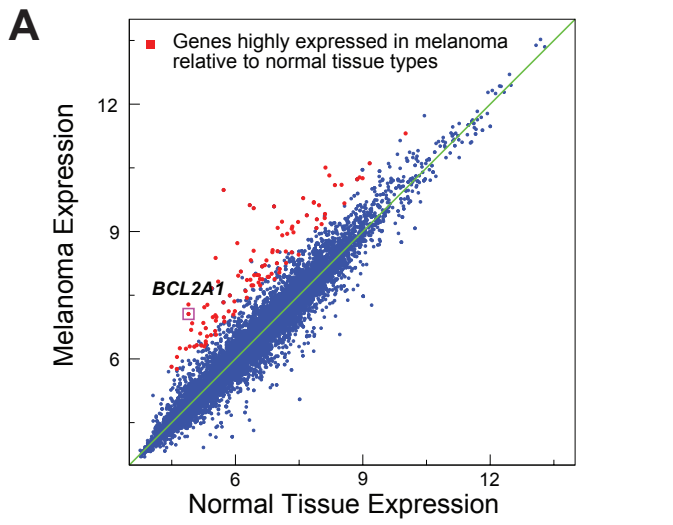


Figure S2

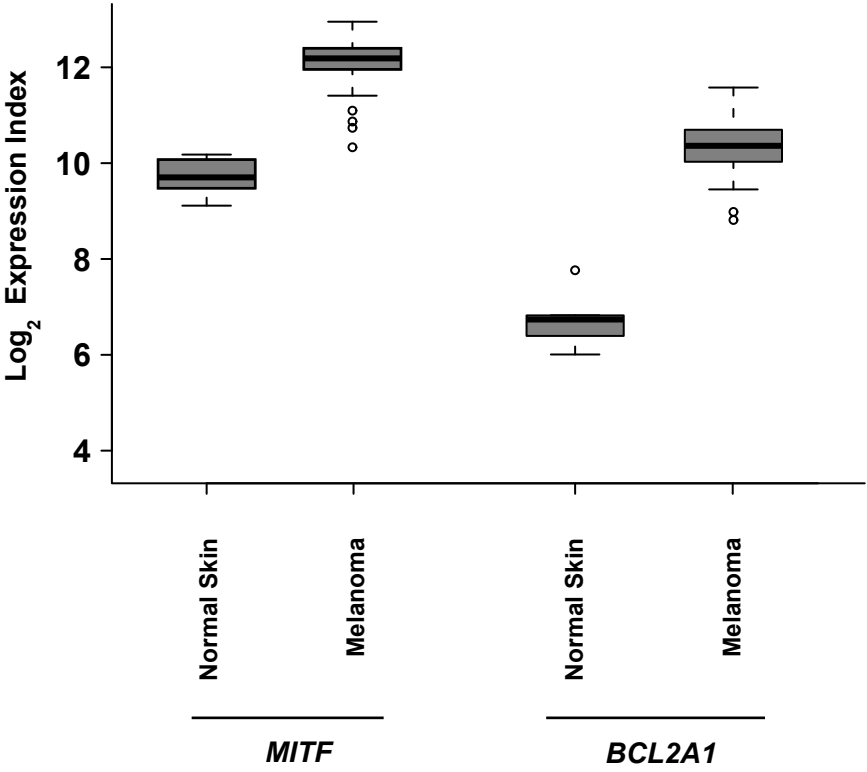
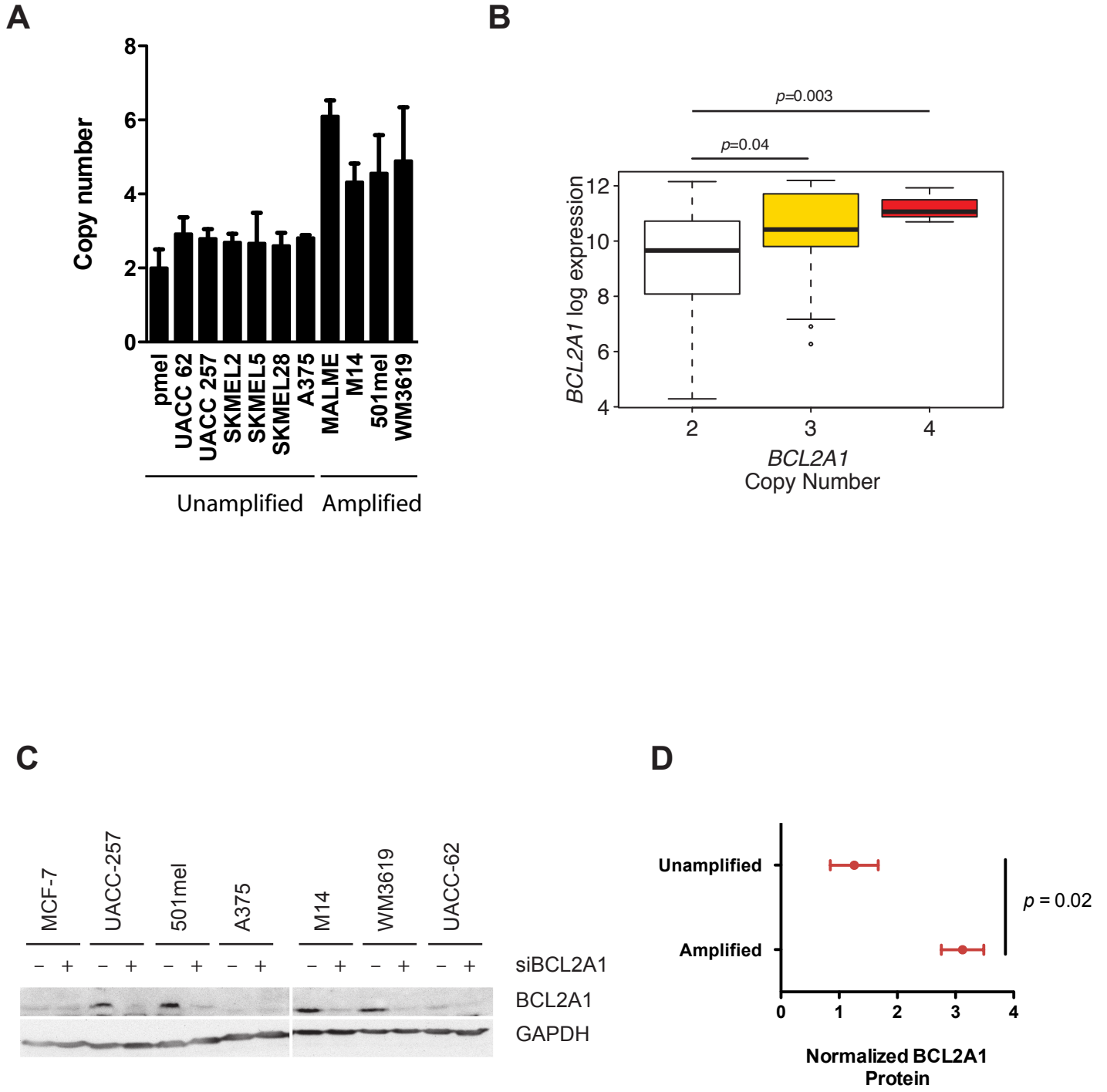
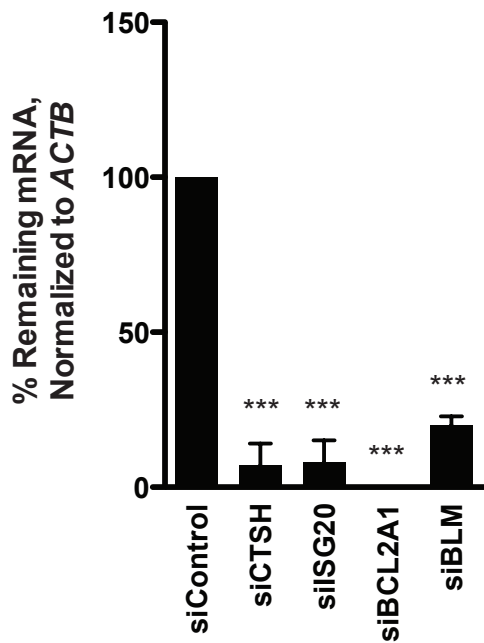


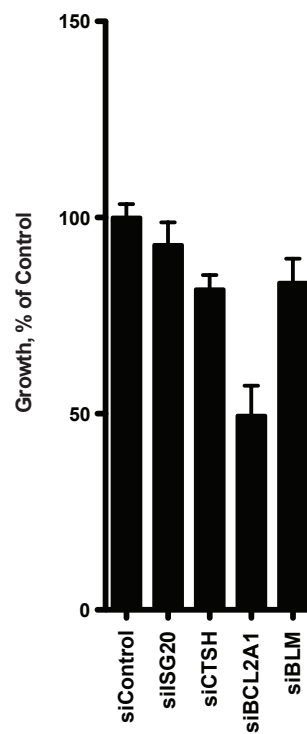
Figure S3



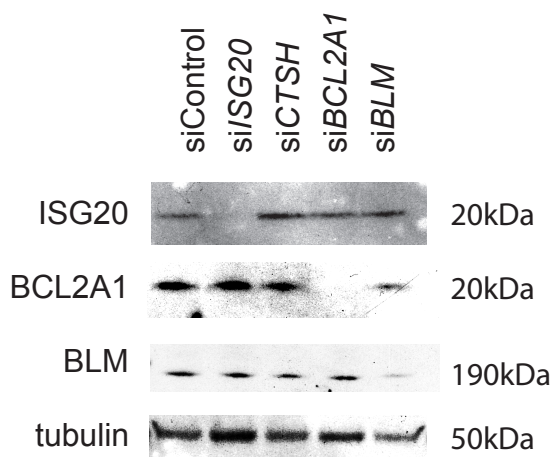
**A**



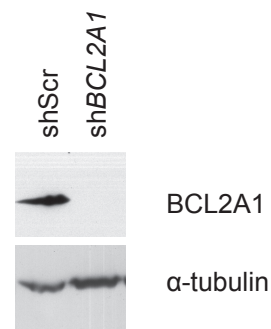
**C**



**B**

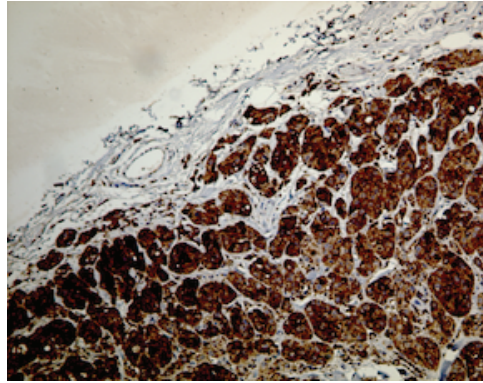


**D**

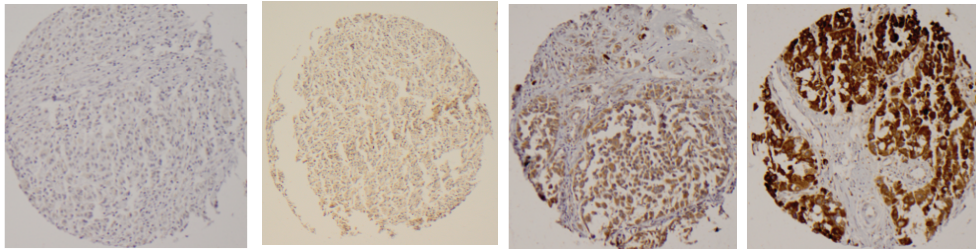


A

Anti-BCL2A1



B



0

1

2

3

Staining Intensity



Figure S6

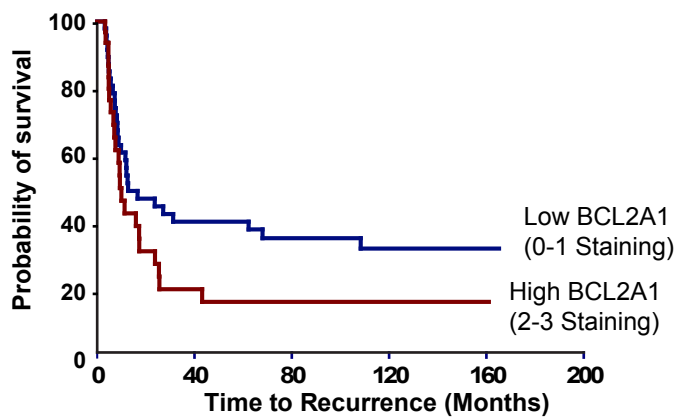
A

<b>Univariate Analysis</b> for <b>BCL2A1</b> <b>(2,3 vs 0,1)</b>	<b>Overall Survival</b> <b>P=0.0042</b>	<b>Disease Free Survival</b> <b>P=0.129</b>	<b>Disease Specific Survival</b> <b>P=0.0064</b>
--	--	--	---

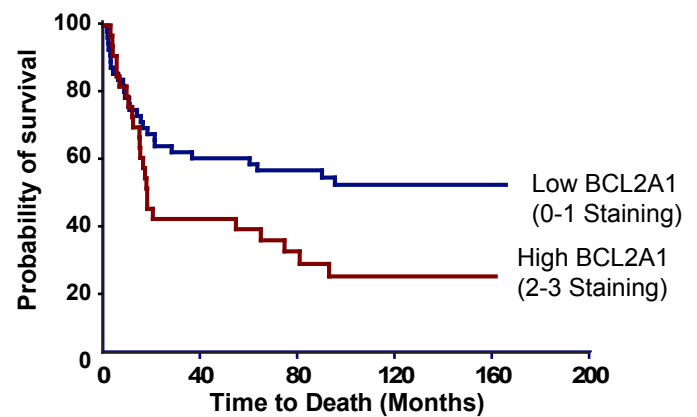
**Multivariate Analysis**

Outcome variable	variable	Total	Failed	Univariate P value (Log Rank Test)	Multivariate HR (95% CI) Cox PH Model	Multivariate P value Cox PH Model
DFS	Ulceration: yes vs no	103	64	0.2833	-	-
	Age: >50 vs ≤50	158	97	0.1514	-	-
	# Positive LN					0.0532 (Type III)
	2-3 vs 1	138	86	0.0498	1.11 (0.64, 1.91)	0.7145
	≥4 vs 1				1.80 (1.09, 2.96)	0.0215
	Marker BCL2A1: 2,3 vs 0,1	158	97	0.129	-	-
DSP	Ulceration: yes vs no	105	69	0.1483	-	-
	Age: >50 vs ≤50	158	101	0.0744	-	-
	# Positive LN					0.0002 (Type III)
	2-3 vs 1	138	85	<.0001	1.37 (0.72, 2.60)	0.3350
	≥4 vs 1				2.84 (1.69, 4.78)	<.0001
	Marker BCL2A1: 2,3 vs 0,1	158	101	0.0064	1.73 (1.06, 2.82)	0.0296

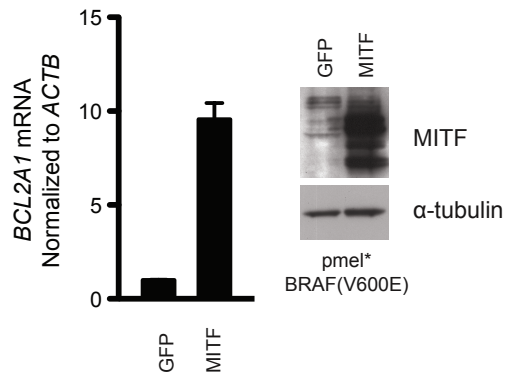
B



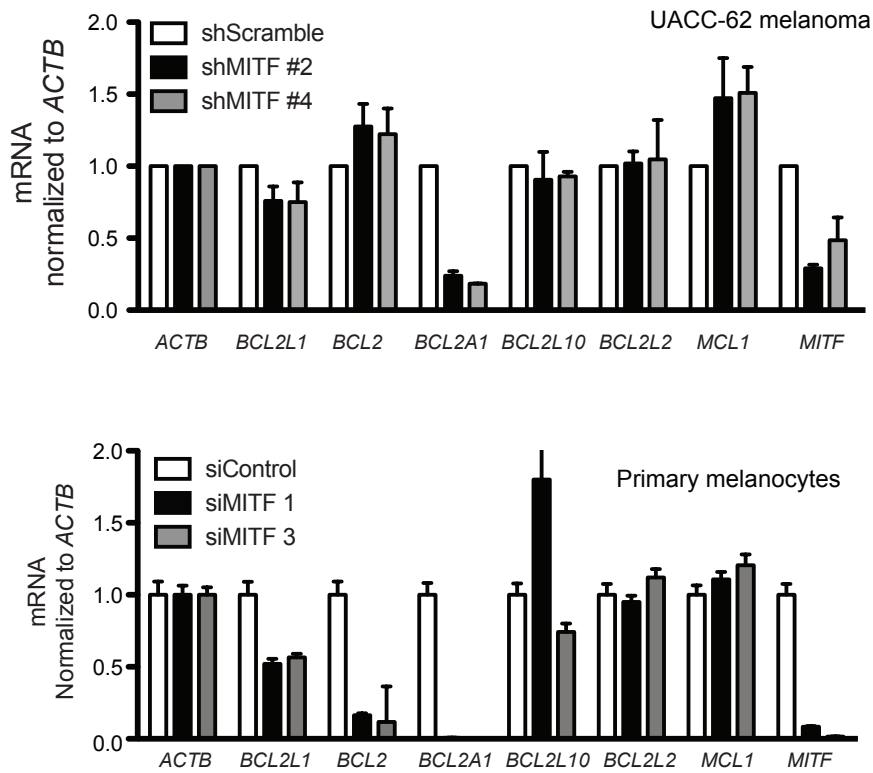
C



**A**



**B**



**C**

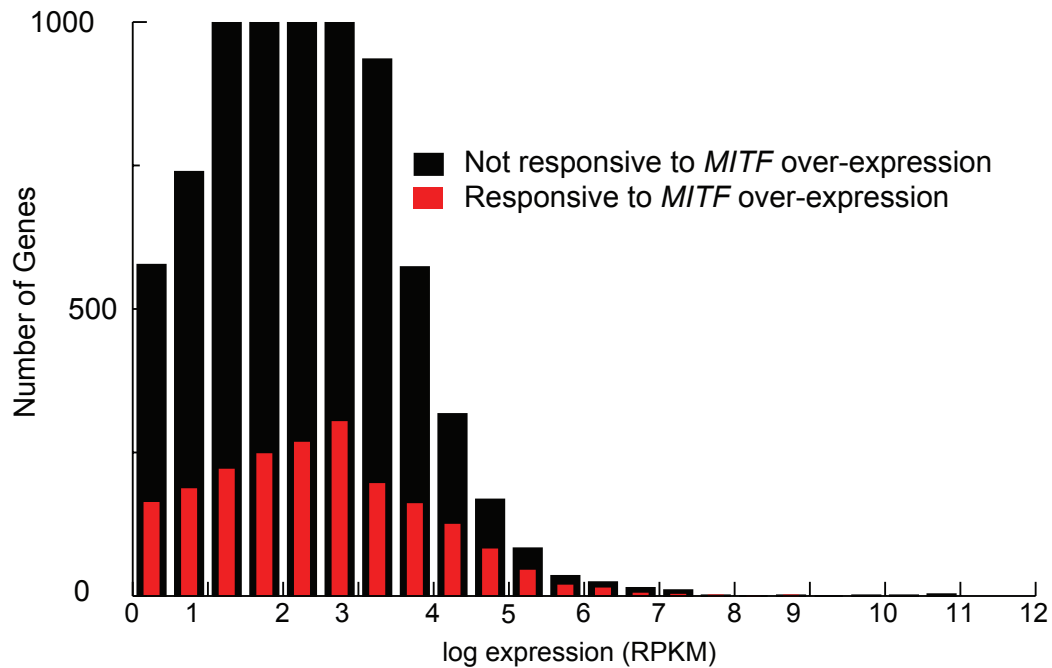




Figure S9

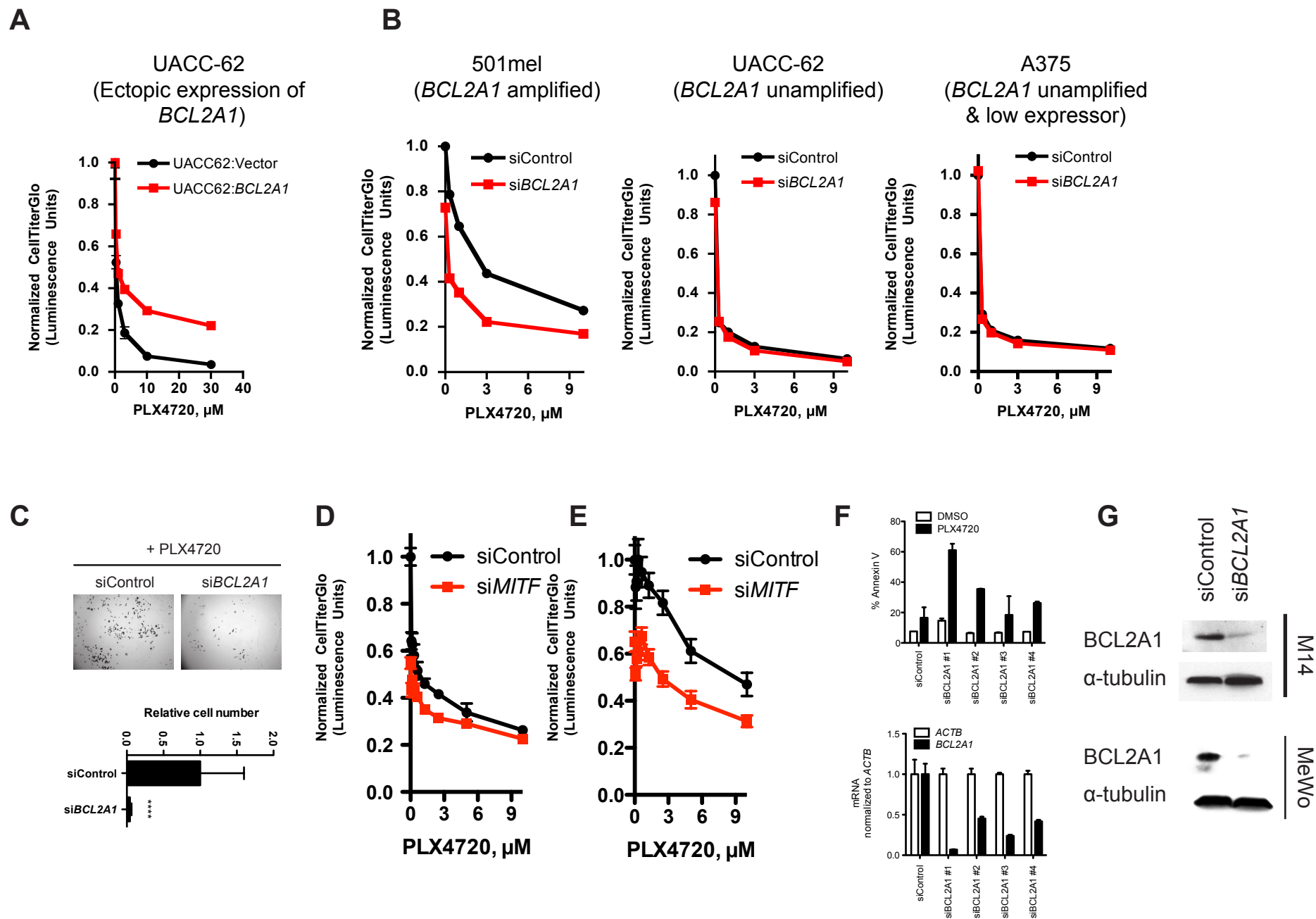
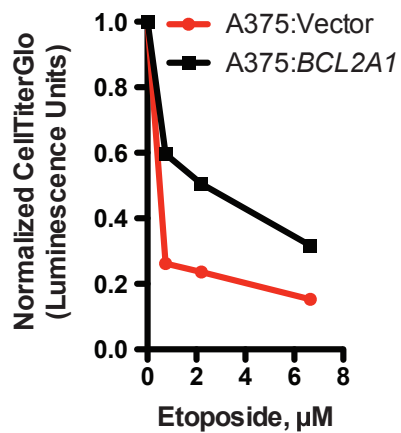
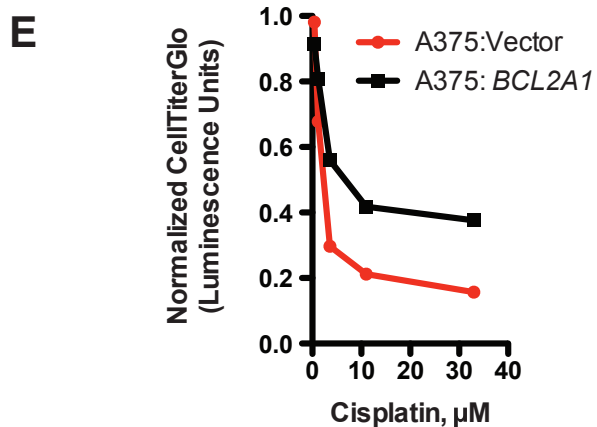
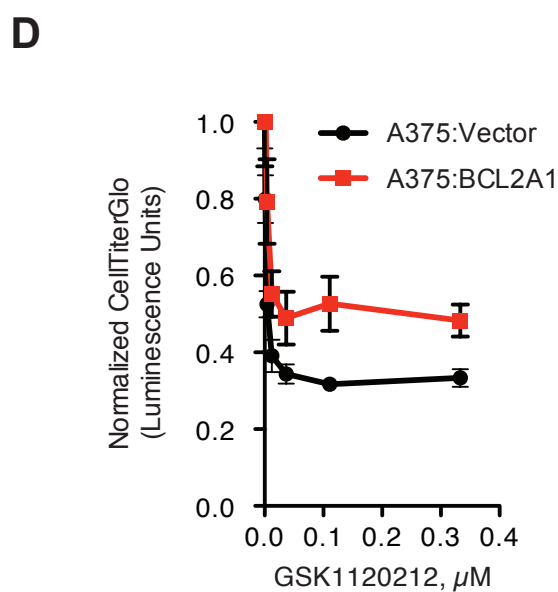
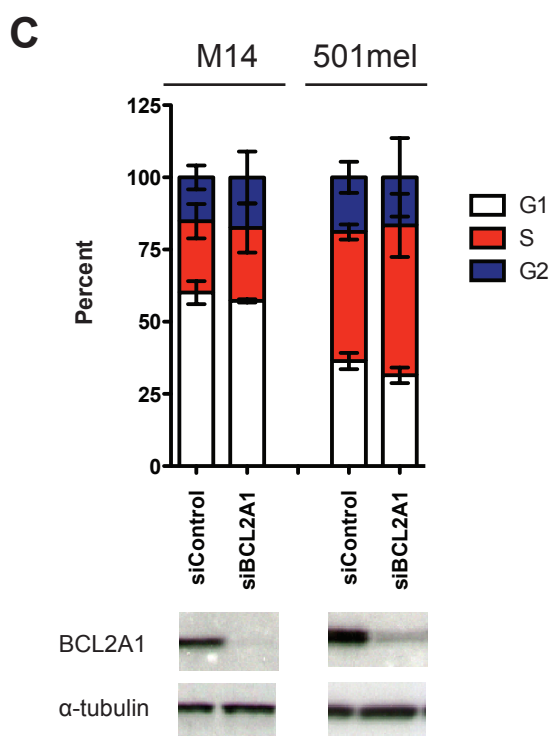
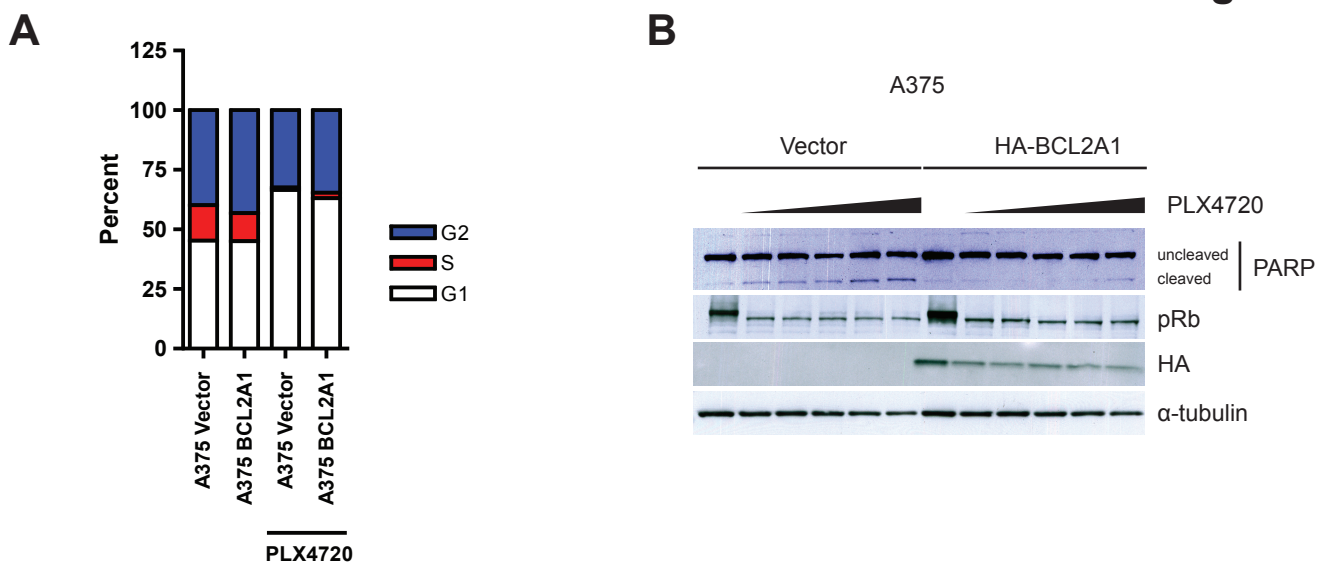
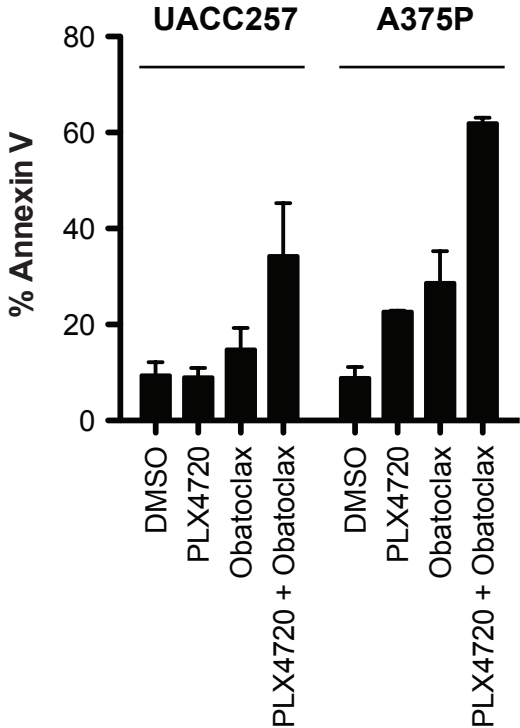


Figure S10



A



B

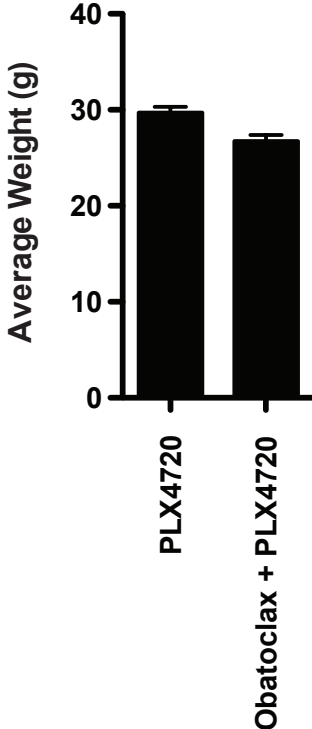


Table S1

<b>Melanoma</b>					
Gene	DEDS q-value	t-statistic	log fold-change	SAM	Moderated-t
ECM1	0	4.901257038	1.704636574	3.51151609	5.582393646
NGS11	0	3.943720102	2.382065773	2.94209027	3.82218504
MITF	0	4.810218334	2.348810196	4.32140064	6.484354973
PLOD3	0	6.594007969	1.500796318	3.43974614	5.832221985
LGALS1	0	5.133096218	1.799913406	2.14137769	2.754107237
BCL2A1	0	2.548150063	1.856725216	2.64086938	3.57996583
S100A1	0	3.438133955	1.688380718	3.59176636	5.815518856
KDELRL3	0	6.01954174	1.677278519	3.05534697	4.56338501
<b>Breast Cancer</b>					
Gene	DEDS q-value	t-statistic	log fold-change	SAM	Moderated-t
RAB25	0	8.97136879	3.415183067	5.40777969	7.069016457
ESRP1	0	9.235303879	2.766311169	5.65729237	8.063433647
CRABP2	0	5.767629623	2.356547356	4.97968674	7.19325161
EPPK1	0	7.566038132	2.200149536	4.77633524	6.979289055
S100A8	0	3.153016567	2.517215252	3.18919039	3.944138527
GATA3	0	4.016681671	2.238086224	4.07236099	5.59243202
TRPS1	0	5.424711227	2.027319908	5.31425905	8.532241821
S100A14	0	4.915256977	2.056806564	3.84265041	5.293976307
SLC2A10	0	4.596642017	2.058450699	3.94063878	5.47672987
EPN3	0	5.70191288	1.892407894	4.88200903	7.7676754
TFAP2C	0	6.75858593	1.811951637	4.82771349	7.824717045
S100A9	0	3.045399189	1.973268509	2.8884449	3.696175098
EFNA1	0	6.02713728	1.695649147	3.62226009	5.256426811
ERBB2	0	3.993111134	1.710947037	3.99184918	6.028445721
SYCP2	0	4.11906147	1.480011463	4.08578157	6.75851049
PBX1	0	4.949214935	1.467093468	3.815413	6.098231792
GRHL2	0	5.285624504	1.439697742	3.77038217	6.050245762
CYB5E1	0	6.777852058	1.278481483	3.83513546	6.711346626
KCNK1	0	4.81363678	1.448740005	3.04234242	4.383326054
TSPYL5	0	2.642868996	1.585701942	2.44767284	3.176804066
LY6E	0	5.460285187	1.28536129	3.06808496	4.685423374
GRB7	0	3.403964281	1.337373734	3.20862412	4.912604809
CCND1	0	3.993065357	1.363913536	2.77497125	3.947113276
F11R	0	6.791478634	1.116340637	3.47728825	6.255654812
<b>Colorectal Cancer</b>					
Gene	DEDS q-value	t-statistic	log fold-change	SAM	Moderated-t
HOXA9	0	8.825346947	2.566873074	6.24113131	9.286178589
KLF5	0	5.324196815	2.198647976	4.55658388	6.346740246
CDX2	0	5.290970325	1.899430275	5.03794098	7.823593616
FERMT1	0	6.600040436	1.823987961	4.6029501	6.97056675
CDH17	0	4.053095341	2.152973175	4.38145447	6.062428474
ABP1	0	4.06414938	2.108811855	4.04558706	5.484385014
DBNDD2	0	6.539642334	1.591943741	3.26074672	4.522328854
SYS1-DBNDD2	0	6.539642334	1.591943741	3.26074672	4.522328854
NFE2L3	0	3.608644247	1.407747269	3.81545377	5.993809223
ESRP1	0	3.525036573	1.630420208	3.15949464	4.297646046
CST3	0	5.627137184	1.554326057	2.82328081	3.760737896
EFNB2	0	4.590442657	1.389659882	3.21938539	4.687995911
HOXA10	0	5.437700272	1.240962982	3.29838872	5.127840042
ADAP1	0	5.247324944	1.084683418	3.40091014	5.837020874
EPS8	0	3.853587627	1.443174362	2.61855245	3.486862421
RAB20	0	4.493474483	1.165225029	3.13509846	4.905637264
TSC22D1	0	4.548624039	1.332318306	2.65872407	3.653202534
EPPK1	0	3.197034597	1.315264702	2.75591207	3.854346514
AGR2	0	2.667286158	1.439027786	2.46045446	3.218842268
DACH1	0	3.059697866	1.158903122	3.08826828	4.807732582
<b>Lung Cancer</b>					
Gene	DEDS q-value	t-statistic	log fold-change	SAM	Moderated-t
FOXA1	0	5.924188614	1.854634285	4.59911823	5.972249985
INSM1	0	4.289059639	1.920189857	3.58472705	4.348173141
TSPYL5	0	4.776727676	1.662230492	3.80129385	4.829018593
ID1	0	4.638103962	1.328636169	3.52009177	4.662004471
ATP1B1	0	4.769937038	1.310111046	3.58316445	4.793656826
ASPH	0	4.788536072	1.217852592	3.53651977	4.827796936
TSPAN13	0	4.30878973	1.168730736	3.22824168	4.332772255
ST18	0	3.766423464	1.200779438	2.94706917	3.81576395
LAPTM4B	0	4.422487259	1.1379776	3.26265144	4.434200764
PFN2	0	4.923530102	1.093223572	3.49218869	4.940559864
GNAI1	0	5.154603004	1.040595055	3.56555438	5.195056975
HRASLS	0	4.40490675	1.058003426	3.20921946	4.450529099
KIAA0895	0	7.065446377	0.953531265	4.25033617	7.137789726
SEPP1	0	2.935031414	1.072528839	2.35708523	2.964581728
SPINT2	0	3.408177137	1.014601707	2.61605263	3.436083555
MBIP	0	7.301733494	0.854499817	4.13721228	7.365073681
PON3	0	4.031141758	0.946343899	2.91965604	4.074910164
FZD6	0	4.626498222	0.89248085	3.15392661	4.659728527
NPTX2	0	3.099447966	0.973684311	2.4128859	3.132674694
FOXG1	0	3.149387121	0.961483479	2.4386878	3.187538862
MLF1	0	4.101799965	0.8856287	2.89186954	4.127875328
B3GALNT1	0	4.161596298	0.877396584	2.92739248	4.216407776
PRKD1	0	4.701046944	0.843999386	3.13858128	4.751564503
<b>Medulloblastoma and Glioblastoma</b>					
Gene	DEDS q-value	t-statistic	log fold-change	SAM	Moderated-t
TWIST1	0	5.486226559	2.750901222	4.83683348	6.609825134
PTN	0	4.766299248	2.338271618	4.53476667	6.423559189
NGS11	0	4.141837597	2.403611183	3.48542356	4.492861271
LRRC17	0	3.535580873	2.120201111	3.76360965	5.160140514
LAMB1	0	5.15025568	1.856568336	2.88095045	3.784554005
CALD1	0	4.747846603	1.766241074	2.93837714	3.942723513
COL1A2	0	2.305601597	1.907495022	2.51067424	3.158425331
GNAI1	0	6.130955696	1.299706459	2.82300806	4.195480347

# Table S2

Name	Description
205681_at	<b>BCL2-related protein A1, BCL2A1</b>
206245_s_at	influenza virus NS1A binding protein, IVNS1ABP
201780_s_at	ring finger protein 13, RNF13
203004_s_at	myocyte enhancer factor 2D, MEF2D
212098_at	hypothetical LOC151162, LOC151162
209736_at	SRY (sex determining region Y)-box 13, SOX13
218343_s_at	general transcription factor IIIC, polypeptide 3, 102kDa, GTF3C3
218152_at	high-mobility group 20A, HMG20A
201779_s_at	ring finger protein 13, RNF13
212534_at	CDNA FLJ11904 fis, clone HEMBB1000048, ---
202618_s_at	methyl CpG binding protein 2 (Rett syndrome), MECP2
203412_at	leucine zipper-like transcription regulator 1, LZTR1
201353_s_at	bromodomain adjacent to zinc finger domain, 2A, BAZZA
203536_s_at	cytosolic iron-sulfur protein assembly 1 homolog (S. cerevisiae), CIAO1
207233_s_at	<b>microphthalmia-associated transcription factor, MITF</b>
209842_at	SRY (sex determining region Y)-box 10, SOX10
214879_x_at	upstream transcription factor 2, c-fos interacting, USF2
203291_at	CCR4-NOT transcription complex, subunit 4, CNOT4
216975_x_at	neuronal PAS domain protein 1, NPAS1
210533_at	catenin (cadherin-associated protein), beta 1, 88kDa, CTNNB1
35160_at	LIM domain binding 1, LDB1
217861_s_at	prolactin regulatory element binding, PREB
217945_at	BTB (POZ) domain containing 1, BTBD1
217501_at	cytosolic iron-sulfur protein assembly 1 homolog (S. cerevisiae), CIAO1
211013_x_at	promyelocytic leukemia, PML
210962_s_at	A kinase (PRKA) anchor protein (yotiao) 9, AKAP9
201362_at	influenza virus NS1A binding protein, IVNS1ABP
211117_x_at	estrogen receptor 2 (ER beta), ESR2
203247_s_at	zinc finger protein 24, ZNF24
212803_at	NGFI-A binding protein 2 (EGR1 binding protein 2), NAB2
201480_s_at	suppressor of Ty 5 homolog (S. cerevisiae), SUPT5H
211049_at	T-cell leukemia homeobox 2, TLX2
218184_at	tubby like protein 4, TULP4
210977_s_at	heat shock transcription factor 4, HSF4
201363_s_at	influenza virus NS1A binding protein, IVNS1ABP
206503_x_at	promyelocytic leukemia, PML
203348_s_at	ets variant gene 5 (ets-related molecule), ETV5
203010_at	signal transducer and activator of transcription 5A, STAT5A
216986_s_at	interferon regulatory factor 4, IRF4
210669_at	transcription factor AP-2 alpha (activating enhancer binding protein 2 alpha), TFAP2A
200677_at	pituitary tumor-transforming 1 interacting protein, PTTG1IP
210697_at	zinc finger protein 257, ZNF257
200037_s_at	chromobox homolog 3 (HP1 gamma homolog, Drosophila) /// similar to chromobox homolog 3, CBX3 /// LOC653972
211014_s_at	promyelocytic leukemia /// hypothetical protein LOC161527, LOC161527 /// PML
203577_at	general transcription factor IIH, polypeptide 4, 52kDa /// valyl-tRNA synthetase 2, mitochondrial (putative), GTF2H4 /// VARS2
220443_s_at	ventral anterior homeobox 2, VAX2
210291_s_at	zinc finger protein 174, ZNF174
207125_at	zinc finger protein 225, ZNF225
210044_s_at	lymphoblastic leukemia derived sequence 1, LYL1
212418_at	E74-like factor 1 (ets domain transcription factor), ELF1
215737_x_at	upstream transcription factor 2, c-fos interacting, USF2
206663_at	Sp4 transcription factor, SP4
213966_at	High-mobility group 20B, HMG20B
215676_at	BRF1 homolog, subunit of RNA polymerase III transcription initiation factor IIIb (S. cerevisiae), BRF1
211118_x_at	estrogen receptor 2 (ER beta), ESR2
205993_s_at	T-box 2, TBX2
206230_at	LIM homeobox 1, LHX1
209778_at	thyroid hormone receptor interactor 11, TRIP11
206202_at	mesenchyme homeobox 2, MEOX2
222136_x_at	zinc finger protein 43, ZNF43
206705_at	tubby like protein 1, TULP1
220714_at	PR domain containing 14, PRDM14
206430_at	caudal type homeobox 1, CDX1
210146_at	nuclear factor (erythroid-derived 2)-like 2, NFE2L2
211524_at	nuclear factor of kappa light polypeptide gene enhancer in B-cells 2 (p49/p100), NFkB2
220804_s_at	tumor protein p73, TP73
217864_s_at	protein inhibitor of activated STAT, 1, PIAS1
213014_at	mitogen-activated protein kinase 8 interacting protein 1, MAPK8IP1
201989_s_at	cAMP responsive element binding protein-like 2, CREBL2
218452_at	SWI/SNF related, matrix associated, actin dependent regulator of chromatin, subfamily a-like 1, SMARCAL1
221321_s_at	Kv channel interacting protein 2, KCNIP2
221557_s_at	lymphoid enhancer-binding factor 1, LEF1
215098_at	retinoid X receptor, beta, RXRB
217069_at	myeloid/lymphoid or mixed-lineage leukemia 4, MLL4
210771_at	peroxisome proliferator-activated receptor alpha, PPARA
206931_at	zinc finger protein 141, ZNF141
206699_x_at	neuronal PAS domain protein 1, NPAS1
206684_s_at	activating transcription factor 7, ATF7
215551_at	estrogen receptor 1, ESR1
221302_at	Kruppel-like factor 15, KLF15
222172_at	neuronal PAS domain protein 3, NPAS3
205861_at	Spi-B transcription factor (Spi-1/PU.1 related), SPIB
206596_s_at	neural retina leucine zipper, NRL
203003_at	myocyte enhancer factor 2D, MEF2D
201184_s_at	chromodomain helicase DNA binding protein 4, CHD4
200877_at	chaperonin containing TCP1, subunit 4 (delta), CCT4
208830_s_at	suppressor of Ty 6 homolog (S. cerevisiae), SUPT6H
205855_at	zinc finger protein 197, ZNF197
220019_s_at	zinc finger protein 224, ZNF224
207936_x_at	ret finger protein-like 3, RFPL3
220025_at	T-box, brain, 1, TBR1
206822_s_at	l(3)mbt-like (Drosophila), L3MBTL
207451_at	NK2 homeobox 8, NKX2-8
217076_s_at	homeobox D3, HOXD3
203349_s_at	ets variant gene 5 (ets-related molecule), ETV5
206379_at	eyes absent homolog 3 (Drosophila), EYA3
207398_at	homeobox D13, HOXD13
208262_x_at	Mediterranean fever, MEFV



Table S3

BRAF status of cell lines used for in vitro and in vitro experiments

<b>Cell line</b>	<b>Tissue</b>	<b>BRAF mutation</b>	<b>BCL2A1 amplification</b>
501mel	Melanoma	BRAF(V600E)	Amplified
A375	Melanoma	BRAF(V600E)	Not amplified
M14	Melanoma	BRAF(V600E)	Amplified
MALME	Melanoma	BRAF(V600E)	Amplified
MCF7	Breast	Wild-type	Not amplified
SK-MEL-2	Melanoma	Wild-type	Not amplified
SK-MEL-28	Melanoma	BRAF(V600E)	Not amplified
SK-MEL-5	Melanoma	BRAF(V600E)	Not amplified
UACC257	Melanoma	BRAF(V600E)	Not amplified
UACC62	Melanoma	BRAF(V600E)	Not amplified
WiDr	Colon	BRAF(V600E)	Not amplified
WM1720	Melanoma	BRAF(V600E)	Amplified
WM3526	Melanoma	BRAF(V600E)	Amplified
WM3619	Melanoma	Wild-type	Amplified

**Table S4.** Details of treatment of patients biopsied for evaluation of relationship of BCL2A1 expression and clinical response.

<b>Patient ID</b>	<b>Treatment</b>
1	Vemurafenib
2	Vemurafenib
3	Vemurafenib
4	Vemurafenib
5	Vemurafenib
6	GSK112021 + GSK2118436
7	GSK112021 + GSK2118436
8	GSK112021 + GSK2118436
9	GSK112021 + GSK2118436
10	GSK112021 + GSK2118436
11	GSK112021 + GSK2118436
12	GSK112021 + GSK2118436
13	GSK112021 + GSK2118436
14	GSK112021 + GSK2118436
16	GSK112021 + GSK2118436
18	GSK112021 + GSK2118436
22	GSK112021 + GSK2118436
24	Vemurafenib
25	GSK112021 + GSK2118436